

Hardware Obfuscation of Digital FIR Filters

Levent Aksoy[†], Alexander Hepp[‡], Johanna Baehr[‡] and Samuel Pagliarini[†]

[†]Department of Computer Systems, Tallinn University of Technology, Tallinn, Estonia

[‡]Department of Electrical and Computer Engineering, Technical University of Munich, Munich, Germany

Abstract—A finite impulse response (FIR) filter is a ubiquitous block in digital signal processing applications. Its characteristics are determined by its coefficients, which are the intellectual property (IP) for its designer. However, in a hardware efficient realization, its coefficients become vulnerable to reverse engineering. This paper presents a filter design technique that can protect this IP, taking into account hardware complexity and ensuring that the filter behaves as specified only when a secret key is provided. To do so, coefficients are hidden among decoys, which are selected beyond possible values of coefficients using three alternative methods. As an attack scenario, an adversary at an untrusted foundry is considered. A reverse engineering technique is developed to find the chosen decoy selection method and explore the potential leakage of coefficients through decoys. An oracle-less attack is also used to find the secret key. Experimental results show that the proposed technique can lead to filter designs with competitive hardware complexity and higher resiliency to attacks with respect to previously proposed methods.

Index Terms—hardware obfuscation, IP protection, reverse engineering, oracle-less attack, digital FIR filter design.

I. INTRODUCTION

Digital filtering is frequently used in digital signal processing (DSP) applications and finite impulse response (FIR) filters are generally preferred due to their stability and linear phase property [1]. The output of an FIR filter $y(j)$ is equal to $\sum_{i=0}^{N-1} h_i \cdot x(j-i)$, where N is the filter length, h_i is the i^{th} filter coefficient, and $x(j-i)$ is the i^{th} previous filter input with $0 \leq i \leq N-1$. Fig. 1 shows the design of transposed form FIR filter. Note that since coefficients determine the filter behavior, they are actually an intellectual property (IP).

In filter design, on one hand, coefficients can be stored in memory, revealing no information to an adversary at an untrusted foundry. Due to the usage of memory and multipliers, which take two inputs as variables, the hardware complexity is increased in this case. On the other hand, since coefficients are determined beforehand, multipliers, whose one input is a variable and the other is a constant, can be used, enabling high-level and logic synthesis tools to embed coefficients into hardware and reduce its complexity further [2]. In this case, coefficients become vulnerable. For example, after resetting registers and applying a constant 1 value to the filter input, the filter output $y(j)$ is computed as $\sum_{i=0}^j h_i$ in the first $N-1$ clock cycles. Thus, by observing the filter output in $N-1$ clock cycles, each coefficient can be determined as follows:

$$h_i = \begin{cases} y(0), & \text{if } i = 0 \\ y(i) - y(i-1), & \text{otherwise.} \end{cases} \quad (1)$$

Over the years, many efficient techniques have been introduced for the protection of IPs. Among these techniques, logic

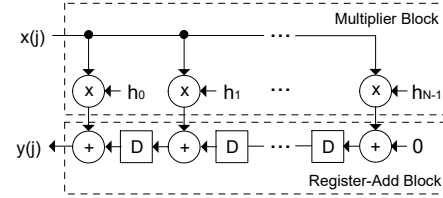


Fig. 1. Parallel transposed form FIR filter design.

locking methods [3] offer a protection against a diverse array of adversaries [4]. They insert additional logic at gate-level, which is driven by a key, so that the circuit behaves as expected only when the secret key is applied. Moreover, high-level obfuscation techniques have been proposed to protect IPs [5]–[7]. In [5], the whole arithmetic function is obfuscated rather than only constants. In [6], constants can be obfuscated by simply replacing their bits by key inputs which are stored in a memory. The obfuscation technique of [7] hides filter coefficients behind decoys. However, since there may exist many possible sets of coefficients that satisfy the filter specification [8], all these methods cannot ensure that the encrypted filter exhibits the specified behavior only when the secret key is provided. To the best of our knowledge, only the approach of [9] can ensure this property using high-level transformations, a key-based finite-state machine, and a reconfigurator.

In this paper, we introduce a filter design technique which obfuscates a digital FIR filter based on the given filter specification. In this technique, the filter behavior is formulated as a linear programming (LP) problem and the filter coefficients, that respect the given filter specification, and their lower and upper bounds are computed. For each filter coefficient, decoy(s) are chosen beyond the lower and upper bounds of the associated coefficient using three alternative decoy selection methods (DSMs). As done in [7], coefficients are protected by hiding them among these decoys using an additional logic with key inputs. This technique can be applied to any type of FIR filter and it works at register-transfer level, enabling logic synthesis tools to reduce the hardware complexity. To find the resiliency of the obfuscated design against an attack at an untrusted foundry, a reverse engineering method based on machine learning is developed to find the DSM and discover possible coefficients among decoys. Also, an oracle-less attack [10] is used to find the secret key. It is shown that the proposed technique using a specific DSM leads to filters with a hardware complexity similar to those obtained by previously proposed methods. However, the attacks are not successful on these proposed designs, while they can discover some coefficients of filters encrypted by other methods.

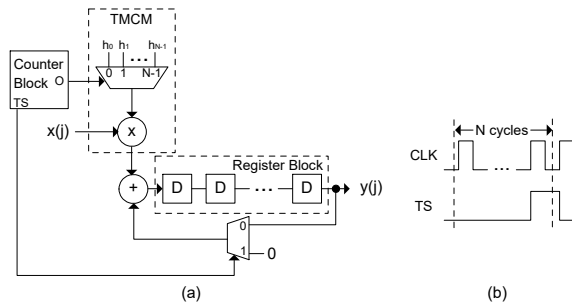


Fig. 2. (a) Folded design of the transposed filter; (b) the timing signal TS .

The remainder of this paper is organized as follows: Section II gives background concepts. The proposed filter design technique is introduced in Section III. Section IV describes the developed reverse engineering technique. Experimental results are given in Section V. Finally, Section VI concludes the paper.

II. BACKGROUND

A. Filter Design

The filter design problem can be defined as finding filter coefficients that satisfy filter constraints based on the filter specification $fspec$, given as a five-tuple, i.e., filter length N , passband w_p and stopband w_s frequencies, and passband δ_p and stopband δ_s ripples [8]. The zero-phase frequency response (ZPFR) of a symmetric FIR filter is given as¹,

$$G(w) = \sum_{i=0}^{\lfloor M \rfloor} e_i h_i \cos(w(M - i)), \quad (2)$$

where $M = (N - 1)/2$, $h_i \in \mathbb{R}$ with $-1 \leq h_i \leq 1$, $w \in \mathbb{R}$ is the angular frequency, and $e_i = 2 - K_{i,M}$ with $K_{i,M}$ is the Kronecker delta². Considering a low-pass filter and assuming that the pass-band and stop-band gains are set to 1 and 0, respectively, the filter must satisfy the following constraints:

$$\begin{aligned} 1 - \delta_p &\leq G(w) \leq 1 + \delta_p, & w \in [0, w_p] \\ -\delta_s &\leq G(w) \leq \delta_s, & w \in [w_s, \pi]. \end{aligned} \quad (3)$$

The filter design problem can be formulated as an LP problem, for which there exists a polynomial-time algorithm [12].

B. Folded Implementation of Digital FIR Filters

After the floating-point filter coefficients are determined, respecting the filter specification, they are converted to integer constants, since floating-point addition and multiplication operations have more hardware complexity than their integer counterparts [13]. Also, the folded design architecture, where computing resources are re-used, is preferred to the parallel design architecture, leading to a significant reduction in area, but increasing the latency of the computation [14].

Fig. 2(a) shows the folded design of the filter given in Fig. 1, where the time-multiplexed constant multiplication (TMCM) block realizes the multiplication of the filter input by a constant selected among all filter coefficients at a time [15]. The register block includes $N - 1$ cascaded registers whose counterparts in

the parallel design are the ones in the register-add block. The $\lceil \log_2 N \rceil$ -bit counter counts from 0 to $N - 1$ and generates the timing signal TS shown in Fig. 2(b). Note that CLK denotes the clock signal fed to all registers which was not shown in Fig. 2(a) for the sake of clarity.

In the proposed filter design technique, the TMCM block including filter coefficients is obfuscated using decoys.

C. Attacker Model for Reverse Engineering

In our threat model, an adversary at an untrusted foundry aims to retrieve coefficients of the FIR filter obfuscated as described in Section III. In this case, it is reasonable to assume that the adversary can identify the block implementing the TMCM operation, either by inspecting the chip data sheet or by using a fuzzy reverse engineering method which labels netlist partitions with their functionality [16]. Thus, the Boolean function of the TMCM block in the netlist is available to the adversary, as well as the implementation details given in Section III. The adversary is assumed to have no further a priori knowledge about the system, such as the filter specification or an unlocked design, and therefore cannot produce an oracle for the filter design. As a consequence, filter coefficients and decoys represent secret information that must be protected. Hence, there must be no information in the netlist that can be used to discern original coefficients from decoys.

III. THE PROPOSED FIR FILTER DESIGN TECHNIQUE

In this section, we present an FIR filter design technique that generates an obfuscated filter whose behavior is the same as the specified one only when the secret key is provided. Its steps are described in detail in the following subsections.

A. Finding Filter Coefficients and Decoys

First, based on the $fspec$, the original filter coefficients are computed by solving the constraints given in Eq. 3.

Second, the lower bound of each coefficient h_i , where $0 \leq i \leq N - 1$, is found by solving the following LP problem:

$$\begin{aligned} \text{minimize : } & cf = h_i \\ \text{subject to : } & 1 - \delta_p \leq G(w) \leq 1 + \delta_p, & w \in [0, w_p] \\ & -\delta_s \leq G(w) \leq \delta_s, & w \in [w_s, \pi] \\ & h^l \leq h \leq h^u, \end{aligned}$$

where cf is the cost function and h^l and h^u are the lower and upper bounds of all filter coefficients which were initially assigned to -1 and 1, respectively. The value of h_i in the LP solution corresponds to its lower bound h_i^l and is stored in a set H^l . Similarly, the upper bound of each coefficient h_i^u is found when $cf = -h_i$ and is stored in a set H^u .

Third, the floating-point coefficients and their lower and upper bounds are converted to integers by multiplying them by 2^Q , where Q is the quantization value, and finding the least integer greater than or equal to this multiplication result.

Fourth, given the number of key inputs p , for each filter coefficient h_i , its decoys are selected beyond its lower and upper bounds as given in Algorithm 1. In its *AssignDecoy* function, decoys are preferred to have the same sign with the

¹The frequency response of an asymmetric filter can be found in [11].

²The $K_{a,b}$ function is 1 when a is equal to b . Otherwise, it is 0.

Algorithm 1 Assignment of decoys to filter coefficients

Given: N , H^l , H^u , and p
 1: $noi = 0$ ▷ Number of iterations
 2: $nok = 0$ ▷ Number of used keys
 3: $D = \{\}$ ▷ Set of arrays including decoys
 4: $nd = \{\}$ ▷ Set including number of decoys
 5: **while** $nok < p$ **do**
 6: $nod = 2^{noi}$ ▷ Number of decoys to be assigned
 7: **for** $i = 0$ **to** $N - 1$ **do**
 8: $(nd_i, D_i) = \text{AssignDecoy}(nod, h_i^l, h_i^u, nd_i, D_i)$
 9: $nok = nok + 1$
 10: **if** $nok == p$ **then**
 11: **break**
 12: $noi = noi + 1$
 13: **return** (nd, D)

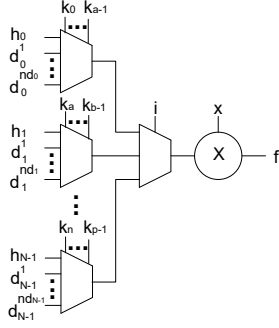


Fig. 3. Obfuscation of the TCMC block.

related filter coefficient to prevent any leakage of information on the original coefficients and are determined to be unique to generate distinct outputs when a wrong key is applied, increasing the output corruption. We consider three DSMs: i) DSM-HD favors decoys with a Hamming distance very close to the related coefficient; ii) DSM-RD chooses decoys randomly whose bit-widths are close to that of the related coefficient; iii) DSM-HDRD, which is a mixture of DSM-HD and DSM-RD, selects a decoy using DSM-HD if the related coefficient is protected by a single decoy, otherwise, chooses decoys using DSM-RD. Note that DSM-HD is introduced to reduce hardware complexity by increasing the sharing of common operations during logic optimization. However, it may lead to a leakage of coefficients when a coefficient has more than one decoy, as shown in Section IV-C. Hence, DSM-RD is proposed to prevent such a leakage. DSM-HDRD is introduced to take advantages of these methods in hardware complexity and resiliency.

B. Realization of the Obfuscated TCMC Block

Fifth, each filter coefficient h_i is hidden among its decoy(s) $D_i = [d_i^1 \dots d_i^{nd_i}]$, where $0 \leq i \leq N - 1$. To do so, a multiplexor (MUX) is used to select the filter coefficient and its decoy(s) using key input(s) k . Locations of a coefficient and its decoys at the MUX inputs are determined randomly. The number of inputs of such a MUX is equal to $nd_i + 1$ and the number of its select inputs is $\lceil \log_2(nd_i + 1) \rceil$. Then, another MUX is used to realize the constant multiplication in the TCMC block in the given order using the primary select input i whose bit-width is $\lceil \log_2 N \rceil$. The number of inputs of this MUX is equal to N . Finally, a multiplier is employed to realize the multiplication of the selected constant by the filter

input x . Its size is equal to $mbw + ibw$, where mbw stands for the maximum bit-width of the filter coefficients and ibw denotes the bit-width of the filter input x . Fig. 3 shows the obfuscated TCMC block. Observe that at least one decoy is multiplied by the filter input under a wrong key. Hence, in a folded design of a filter whose TCMC block is obfuscated using the proposed method, a wrong key always generates a wrong output. Since decoys are selected beyond the possible values of filter coefficients, these wrong outputs lead to a filter behavior other than the specified one.

Finally, the folded FIR filter including the obfuscated TCMC block is implemented as given in Fig. 2(a). A computer-aided design tool is developed to automate the design and verification processes of the obfuscated FIR filter.

IV. THE DEVELOPED REVERSE ENGINEERING METHOD

In this section, we describe an attack on the filter design obfuscated as presented in Section III using reverse engineering. Its steps are described in detail in the following subsections.

A. Identifying the TCMC Block in Obfuscated Filter Design

In the gate-level netlist of an obfuscated FIR filter, its TCMC block can be identified as partitions using a fuzzy reverse engineering method [16]. At the end of this step, the attacker has extracted the netlist, i.e., the Boolean function of the TCMC block, that is used in the next step.

B. Extracting Constants from the TCMC Netlist

Although constants have been embedded into the TCMC design by the synthesis tool during logic optimization, they can be extracted with reverse engineering. Hypotheses for the constants can be built by using an arbitrary multiplication method as an oracle. The aim is to find constants in a way that the multiplication oracle behaves identically to the reverse engineered TCMC block under all possible filter input x for the given primary select input i and key input k . An exhaustive search for constants is not feasible, as it would be necessary to evaluate at most 2^{mbw} combinations for all i and k values. We can instead extract constants efficiently with satisfiability (SAT) solving. Let $f_r(i, k, x)$ denote the n -bit Boolean function of the TCMC block in the netlist. We define $f(c, x) = c \cdot x$ to be the n -bit Boolean function realizing the multiplication of an n -bit constant c by an n -bit input x . Let $r_{i,k}$ denote any reverse-engineered constant for a particular i and k , let $a[0]$ denote the least significant bit (LSBs) of the n -bit constant or function a and let $a[0..j]$ denote the range of bits of a with indices from 0 to j . Thus, to determine the list of constants, we search for $r_{i,k}$ that solves the equation

$$\forall x \quad f(r_{i,k}, x) = f_r(i, k, x).$$

As the LSB of multiplication only depends on the LSBs of $r_{i,k}$ and x , we can begin to search for $r_{i,k}[0]$ that satisfies

$$\forall x[0] \quad f(r_{i,k}[0], x[0])[0] = f_r(i, k, x[0])[0].$$

We subsequently search for $r_{i,k}[j]$, $0 < j < n$, that satisfies

$$\forall x[0..j] \quad f(r_{i,k}[0..j], x[0..j])[j] = f_r(i, k, x[0..j])[j],$$

using the previously calculated $r_{i,k}[0..j-1]$. In this process, the miter logic is constructed as $f \oplus f_r$ and a SAT solver is used to search for an unsatisfying value of $r_{i,k}[j]$ for the miter logic starting from the LSB. Bits of $r_{i,k}$ found in each iteration reduce the search in the next iteration to just one unknown bit. This process is repeated for all values of i and k .

Using the SAT formulation described in this subsection, for each filter coefficient h_i , we obtain the list of all reverse engineered constants $R_i = [r_{i,1}, \dots, r_{i,nd_i+1}]$ including the coefficient and its decoys. As coefficients and decoys are handled equally by MUXes shown in Fig. 3, there is no structural or functional information that allows a discrimination.

C. Vulnerability of the DSM

Depending on the DSM, an element of R_i may be more probable to be h_i . For example, suppose that the original coefficient is 7 $(111)_2$ and 3 decoys, i.e., 6 $(110)_2$, 5 $(101)_2$, and 3 $(011)_2$, are found using DSM-HD. Observe that each decoy has a Hamming distance value of 1 to the original coefficient. However, these decoys actually make it obvious that the original coefficient is 7. Because only for this constant, the Hamming distance to all other constants is always 1.

In order to exploit this vulnerability, it is necessary to differentiate the DSM used in an obfuscated TCMC block. We implemented the structural reverse engineering based method described in [16] and created a library of 7000 synthesized TCMC blocks. In this library, there are 2000 TCMC designs for each DSM and 1000 TCMC designs without decoys. After synthesis, the netlists were parsed from Verilog to a graph representation using pyverilog [17] and networkx [18]. Without compromising accuracy, buffers were removed from the netlists as done in [16]. The graph representation is then converted into a graph embedding using structural properties of the graph as presented in [16]. Each graph embedding is labelled with the DSM used to create the netlist or 0 otherwise. Finally, the XGBClassifier of [19] is trained without scaling and preprocessing. The XGBClassifier is a time and space efficient implementation of a machine learning tool using gradient tree boosting, that is appropriate for the large number of features and learning samples used in this work. To prove the ability of the machine learning tool to identify the DSM for all designs in the library, we performed a 5-fold cross validation with a test size of 20% of all TCMC designs. In the cross validation, on average, excellent macro and micro $f1$ performance scores of 0.99 were achieved for the test sets.

D. Finding Original Coefficients

After the DSM used in the TCMC block is classified, the final step is to find h_i in R_i . To do so, a script, called DOC-HD, is developed to determine h_i based on the observation explained in Section IV-C. We note that neither DSM-RD nor DSM-HDRD are vulnerable to this attack. DSM-RD is not vulnerable, as it does not use the Hamming distance based DSM. DSM-HDRD is not vulnerable, as it does use the Hamming distance based DSM only if there is a single decoy, but in this case, it is equally probable that either $r_{i,k}$ in R_i is the filter coefficient

TABLE I
FIR FILTER SPECIFICATIONS.

Index	Type	N	w_p	w_s	δ_p	δ_s	Q
1	low-pass	29	0.3	0.5	0.00316	0.00316	14
2	low-pass	59	0.125	0.225	0.01	0.001	14
3	high-pass	105	0.8	0.7	0.005	0.001	14

h_i . This particular observation can be formalized as follows. To protect against the entire reverse engineering attack, it is important that the attacker cannot discriminate the reverse engineered constants in R_i . Thus, decoys must be chosen such that there is no information to tell coefficients and decoys apart. This observation leads to the condition

$$\forall d_i^m \quad P_{\text{DSM}}[r_{i,k} = h_i] = P_{\text{DSM}}[r_{i,k} = d_i^m], 1 \leq m \leq nd_i \quad (4)$$

to be held. The probability that the DSM outputs any decoy value must be equal to the probability that the DSM outputs the filter coefficient. In this case, Definition 1 of [20] is fulfilled and the obfuscation scheme becomes provably secure against a reverse engineering based attack *without a priori* knowledge of the filter specification. Eq. 4 holds for DSM-RD, as decoys are selected from a uniform random distribution. It is equally probable that h_i is sampled from the random distribution by DSM-RD. Eq. 4 also holds for DSM-HDRD. If there are multiple decoys for a given coefficient, DSM-HDRD is equal to DSM-RD. If there is a single decoy, it is equally probable for both entries in R_i that one is derived from the other. It can be concluded that while DSM-HD is vulnerable to the reverse engineering attack when a coefficient is protected by multiple decoys, an adversary cannot gain any advantage over brute-forcing the key for DSM-RD and DSM-HDRD.

V. EXPERIMENTAL RESULTS

We used three FIR filters whose specifications are given in Table I. These filters are obfuscated using the proposed technique. Moreover, their TCMC blocks, including the original coefficients, are locked by conventional methods [21], [22] and obfuscated by the technique of [7] using a Hamming distance based DSM similar to DSM-HD. This section presents the synthesis results of encrypted filters, resiliency of encrypted TCMC blocks to reverse engineering and oracle-less [10] attacks, and behavior of encrypted filters.

A. Synthesis of Encrypted Filters

In order to find the hardware complexity of encrypted FIR filters, they are synthesized when the bit-width of the filter input is 32. Note that logic synthesis is performed by Cadence Genus using a commercial 65 nm cell library. The encrypted designs are validated in simulation using 10,000 randomly generated inputs where the collected switching activity data is used to compute power dissipation. Table II presents the gate-level synthesis results of filters encrypted using p key inputs. In this table, *area*, *delay*, and *power* stand for the total area in μm^2 , delay in the critical path in ps , and total power dissipation in μW , respectively. Note that encrypted filters with minimum area are shown in bold.

Observe from Table II that among the logic locking methods, the method of [22] leads to locked filters with the smallest

TABLE II
SYNTHESIS RESULTS OF ENCRYPTED FIR FILTERS.

Index	p	Encryption	Technique	Synthesis Results		
				area	delay	power
1	32	Logic Locking	[21]	14596	5708	1668
			[22]	14452	5423	1428
		Obfuscation	[7]	14483	6599	1545
			OURS - DSM-HD	14475	6123	1523
			OURS - DSM-RD	14818	6625	1672
OURS - DSM-HDRD	14616	5753	1555			
2	64	Logic Locking	[21]	26096	6075	2383
			[22]	25898	6400	2229
		Obfuscation	[7]	25856	6764	2266
			OURS - DSM-HD	25851	6523	2202
			OURS - DSM-RD	26146	6598	2248
OURS - DSM-HDRD	25949	6563	2249			
3	128	Logic Locking	[21]	45466	7072	3979
			[22]	45404	7179	3840
		Obfuscation	[7]	45387	7321	3882
			OURS - DSM-HD	45437	6976	3837
			OURS - DSM-RD	46059	6458	3901
OURS - DSM-HDRD	45690	7383	3927			

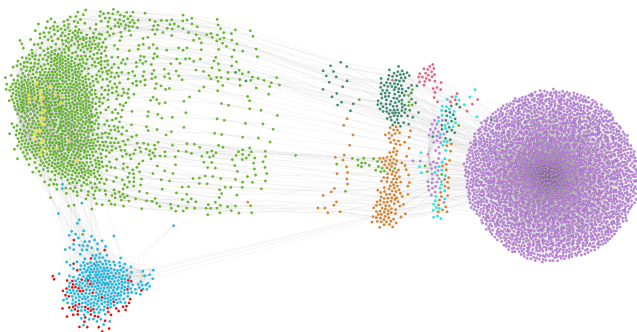


Fig. 4. Netlist graph of identified blocks in the obfuscated filter.

area, achieving a maximum of 2.71% gain in area with respect to the method of [21]. Also, among the obfuscation techniques, the technique of [7] and the proposed technique using DSM-HD leads to obfuscated filters with the smallest area, while the filters obfuscated by the proposed technique using DSM-RD have the largest area. In this case, the gain in area reaches up to 2.31% when compared to the proposed technique using DSM-RD. This is because while DSM-HD uses decoys whose Hamming distance to the filter coefficients is the smallest, DSM-RD favors random decoys. Also, the proposed technique using DSM-HD and DSM-HDRD generates filters with hardware complexity very close to each other, since DSM-HDRD uses decoys, whose Hamming distance to each coefficient is the smallest, for coefficients protected by a single decoy. Note also that there exist obfuscated filters that occupy less area than locked filters, e.g., Filters 2 and 3.

B. Attacks to Encrypted TCM Blocks

1) *Reverse Engineering*: Fig. 4 shows the blocks of Filter 2 obfuscated by the proposed technique using DSM-HD which are identified by the reverse engineering method of [16]. Note that while the yellow and red dots denote the filter inputs and key inputs, respectively, the cyan dots denote the filter outputs. Also, the bright and light green dots represent the multiplier and adder, respectively. The other dots denote the glue logic.

Table III shows the results on the reverse engineering attack, in which acc is the probability that the design is obfuscated by a Hamming distance based DSM, as reported by the XGB-

TABLE III
RESULTS OF THE REVERSE ENGINEERING ATTACK ON OBFUSCATED TCM BLOCKS.

Index	p	Technique	Attack Results			
			acc	vc	cdc	apc
1	32	[7]	0.9986	3	3	2^{26}
		OURS - DSM-HD	0.8896	3	3	2^{26}
		OURS - DSM-RD	0.0086	NA	NA	2^{32}
		OURS - DSM-HDRD	0.9869	3	0	2^{32}
2	64	[7]	0.9999	5	5	2^{54}
		OURS - DSM-HD	0.9999	5	5	2^{54}
		OURS - DSM-RD	0.9991	5	0	2^{64}
		OURS - DSM-HDRD	0.9998	5	0	2^{64}
3	128	[7]	0.9999	23	23	2^{82}
		OURS - DSM-HD	0.9999	23	23	2^{82}
		OURS - DSM-RD	0.0009	NA	NA	2^{128}
		OURS - DSM-HDRD	0.9883	23	0	2^{128}

TABLE IV
RESULTS OF THE ORACLE-LESS ATTACK ON ENCRYPTED TCM BLOCKS.

Index	p	Encryption	Technique	Attack Results		
				dk	pcdk	time
1	32	Logic Locking	[21]	3	100	5.35
			[22]	32	100	4.94
		Obfuscation	[7]	32	53.1	5.27
			OURS - DSM-HD	32	62.5	5.31
			OURS - DSM-RD	32	62.6	3.32
OURS - DSM-HDRD	32	50	6.04			
2	64	Logic Locking	[21]	8	50	9.27
			[22]	64	100	10.07
		Obfuscation	[7]	64	51.6	9.45
			OURS - DSM-HD	64	59.3	9.73
			OURS - DSM-RD	63	57.1	6.59
OURS - DSM-HDRD	64	53.1	10.08			
3	128	Logic Locking	[21]	19	68.4	21.61
			[22]	128	100	23.43
		Obfuscation	[7]	128	63.2	22.11
			OURS - DSM-HD	128	63.2	21.1
			OURS - DSM-RD	128	64	16
OURS - DSM-HDRD	128	50	27.76			

Classifier, vc is the number of vulnerable coefficients, actually the number of coefficients protected by multiple decoys, and cdc is the number of correctly determined coefficients found by the DOC-HD script described in Section IV-D. Note that this script is not applicable (NA) to DSMs with an acc value close to 0. Finally, apc is the number of all possible combinations of constants to be tried to find coefficients.

Observe from Table III that a Hamming distance based DSM can be found with a high accuracy, except DSM-RD on Filter 2. The vulnerable coefficients are easily identified in TCM blocks obfuscated by the technique of [7] and the proposed technique using DSM-HD, reducing the effort of the attacker on exhaustive search of filter coefficients. As DSM-HDRD selects a single decoy for a coefficient using DSM-HD, it is correctly classified as a Hamming distance based DSM. Still, DOC-HD fails to identify the coefficients, as DSM-HDRD selects these multiple decoys randomly for a coefficient using DSM-RD.

2) *Oracle-less Attack*: The attack of [10] is used to find the secret key of encrypted TCM blocks. Table IV presents its solutions, where dk and $pcdk$ stand for the number of deciphered key inputs and the percentage of correct deciphered key bits, respectively and $time$ denotes its run-time in seconds.

Observe from Table IV that the oracle-less attack can decipher a small number of key inputs of designs locked by the technique of [21] with a high accuracy, except Filter 2. It can determine the secret key of designs locked by the technique

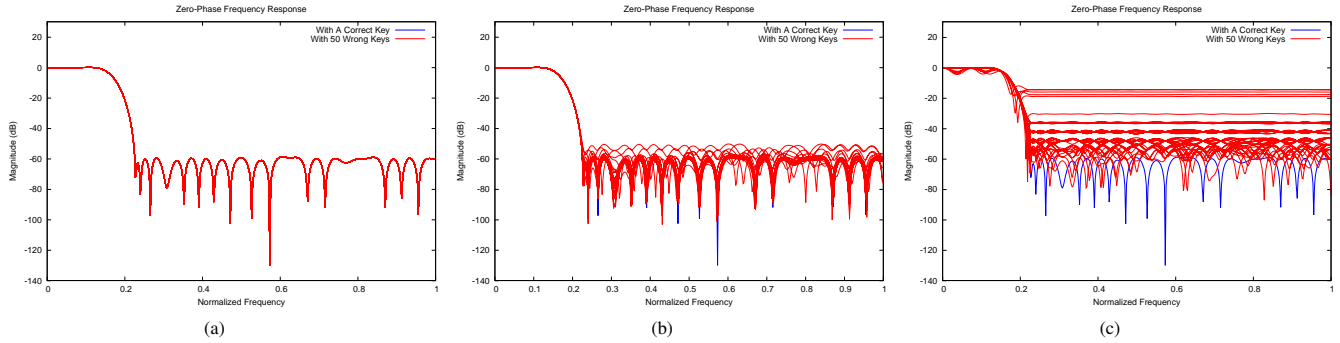


Fig. 5. ZPFrs of FIR filters: (a) locked by the method of [22]; (b) obfuscated by the method of [7]; (c) obfuscated by the proposed method using DSM-HDRD.

of [22]. In contrast, its guesses on the key inputs of obfuscated designs are slightly better than a random guess.

C. Filter Behavior

In order to find the behavior of an encrypted FIR filter, Filter 2 is considered. The ZPFR of an encrypted filter given in Eq. 2 is computed based on the filter coefficients determined as given in Eq. 1 after applying a specific filter input and observing the filter output. Fig. 5 presents ZPFrs of filters locked by the method of [22], obfuscated by the technique of [7] and the proposed technique using DSM-HDRD. The filter behavior is obtained using 50 wrong keys, which are very close to the secret key in terms of the Hamming distance.

Observe from Fig. 5 that while the filter locked by the method of [22] has the original filter behavior under the given wrong keys, the filter obfuscated by the technique of [7] has a behavior very similar to the original one under some wrong keys. In contrast, the filter obfuscated by our proposed technique exhibits incorrect behavior under every wrong key. We note that this property is also observed on filters obfuscated by the proposed technique using DSM-HD and DSM-RD. Observe from Tables II-IV that the proposed technique using DSM-HDRD generates filters with competitive hardware complexity and high security.

VI. CONCLUSIONS

This paper presented a filter design technique, which can obfuscate an FIR filter such that it exhibits a correct behavior only when the secret key is provided. It also introduced a reverse engineering technique to determine the original filter coefficients through selected decoys. The proposed obfuscation technique was compared to conventional logic locking methods and a recently proposed obfuscation technique. It was shown that it can generate filters whose hardware complexity is very close to those of filters encrypted by previously proposed techniques. However, filters obfuscated by our proposed technique present better security properties.

ACKNOWLEDGMENT

This work was partially supported by the EC through the European Social Fund in the context of the project "ICT programme". It was also partially supported by European Union's Horizon 2020 research and innovation programme under grant agreement No 952252 (SAFEST).

REFERENCES

- [1] L. Wanhammar, *DSP Integrated Circuits*. Academic Press, 1999.
- [2] L. Aksoy, P. Flores, and J. Monteiro, "A Tutorial on Multiplierless Design of FIR Filters: Algorithms and Architectures," *Circuits, Syst., Signal Process.*, vol. 33, no. 6, p. 1689–1719, 2014.
- [3] S. Dupuis and M.-L. Flottes, "Logic Locking: A Survey of Proposed Methods and Evaluation Metrics," *J. Electron. Testing*, vol. 35, pp. 273–291, 2019.
- [4] M. Yasin, A. Sengupta, M. T. Nabeel, M. Ashraf, J. Rajendran, and O. Sinanoglu, "Provably-Secure Logic Locking: From Theory To Practice," in *ACM SIGSAC CCCS*, 2017, p. 1601–1618.
- [5] S. A. Islam, L. K. Sah, and S. Katkoori, "High-Level Synthesis of Key-Obfuscated RTL IP with Design Lockout and Camouflaging," *ACM TODAES*, vol. 26, no. 1, 2020.
- [6] C. Pilato, A. Chowdhury, D. Sciuto, S. Garg, and R. Karri, "ASSURE: RTL Locking Against an Untrusted Foundry," *IEEE TVLSI*, vol. 29, no. 7, pp. 1306–1318, 2021.
- [7] L. Aksoy et al., "High-Level Intellectual Property Obfuscation via Decoy Constants," in *IOLTS*, 2021, pp. 1–7.
- [8] L. Aksoy, P. Flores, and J. Monteiro, "Exact and Approximate Algorithms for the Filter Design Optimization Problem," *IEEE TSP*, vol. 63, no. 1, pp. 142–154, 2015.
- [9] Y. Lao and K. K. Parhi, "Obfuscating DSP Circuits via High-Level Transformations," *IEEE TVLSI*, vol. 23, no. 5, pp. 819–830, 2015.
- [10] A. Alaql, M. Rahman, and S. Bhunia, "SCOPE: Synthesis-Based Constant Propagation Attack on Logic Locking," *IEEE TVLSI*, pp. 1–14, 2021.
- [11] Y. C. Lim, "Design of Discrete-Coefficient-Value Linear Phase FIR Filters with Optimum Normalized Peak Ripple Magnitude," *IEEE TCAS*, vol. 37, no. 12, pp. 1480–1486, 1990.
- [12] G. Dantzig, *Linear Programming and Extensions*. Princeton University Press, 1963.
- [13] M. Horowitz, "Computing's Energy Problem (and what we can do about it)," in *IEEE Int. Solid-State Circuits Conf.*, 2014.
- [14] K. Parhi, *VLSI Digital Signal Processing Systems: Design and Implementation*. John Wiley & Sons, 1999.
- [15] L. Aksoy, P. Flores, and J. Monteiro, "Multiplierless Design of Folded DSP Blocks," *ACM TODAES*, vol. 20, no. 1, 2014.
- [16] J. Baehr, A. Bernardini, G. Sigl, and U. Schlichtmann, "Machine Learning and Structural Characteristics for Reverse Engineering," *Integration*, vol. 72, pp. 1–12, 2020.
- [17] S. Takamaeda-Yamazaki, "Pyverilog: A Python-Based Hardware Design Processing Toolkit for Verilog HDL," in *Appl. Reconfigurable Comput.*, 2015.
- [18] A. Hagberg, D. Schult, and P. Swart, "Exploring Network Structure, Dynamics, and Function using NetworkX," in *SciPy*, 2008, pp. 11–15.
- [19] T. Chen and C. Guestrin, "XGBoost: A Scalable Tree Boosting System," in *Int. Conf. Knowl. Discovery Data Mining*, 2016, p. 785–794.
- [20] M. E. Massad, J. Zhang, S. Garg, and M. V. Tripunitara, "Logic Locking for Secure Outsourced Chip Fabrication: A New Attack and Provably Secure Defense Mechanism," 2017. [Online]. Available: <http://arxiv.org/abs/1703.10187>
- [21] J. A. Roy, F. Koushanfar, and I. L. Markov, "EPIC: Ending Piracy of Integrated Circuits," in *DATE*, 2008, pp. 1069–1074.
- [22] M. Yasin, B. Mazumdar, J. J. V. Rajendran, and O. Sinanoglu, "SAR-Lock: SAT Attack Resistant Logic Locking," in *HOST*, 2016, pp. 236–241.